

AD A110159

DTIC FILE COPY

LEVEL III

(12)

NRTC 82-2R

NR 395-706/DARPA Order 3125 AM #15

A100677

SCALING STUDIES OF EFFICIENT  
RAMAN CONVERTERS

(12) 54

H. Kamine  
NORTHROP CORPORATION  
Northrop Research and Technology Center  
One Research Park  
Palos Verdes Peninsula, California 90274

DTIC  
ELECTE  
JAN 27 1982  
S D E

December 1981

Technical Report Covering the Period  
21 March 1980 through 20 March 1981

Prepared for:

DEFENSE ADVANCED RESEARCH  
PROJECTS AGENCY  
1400 Wilson Blvd.  
Arlington, Virginia 22209

407696

This document has been approved  
for public release and sale; its  
distribution is unlimited.

01 27 81 068

The views and conclusions contained in this document are those of the authors and should not be interpreted as necessarily representing the official policies, either expressed or implied, of the Defense Advanced Research Projects Agency or the U.S. Government.

REPORT DOCUMENTATION PAGE		READ INSTRUCTIONS BEFORE COMPLETING FORM	
1. REPORT NUMBER NRTC-82-2R ✓	2. GOVT ACCESSION NO. AD-A110159	3. RECIPIENT'S CATALOG NUMBER	
4. TITLE (and Subtitle)  Scaling Studies of Efficient Raman Converters		5. TYPE OF REPORT & PERIOD COVERED  Final Report	
		6. PERFORMING ORG. REPORT NUMBER	
7. AUTHOR(s)  H. Komine, E. A. Stappaerts, S. J. Brosnan and J. B. West		8. CONTRACT OR GRANT NUMBER(s)  N00014-80-C-0442 DARPA D110159	
9. PERFORMING ORGANIZATION NAME AND ADDRESS Northrop Research and Technology Center One Research Park Palso Verdes Peninsula, CA 90274		10. PROGRAM ELEMENT, PROJECT, TASK AREA & WORK UNIT NUMBERS	
11. CONTROLLING OFFICE NAME AND ADDRESS Defense Advanced Research Projects Agency 1400 Wilson Blvd. Arlington, VA 22209		12. REPORT DATE 12-1-81	
		13. NUMBER OF PAGES	
14. MONITORING AGENCY NAME & ADDRESS (if different from Controlling Office) Office of Naval Research Western Regional Office 1030 East Green St Pasadena, CA 91106		15. SECURITY CLASS. (of this report)  UNCLASSIFIED	
		15a. DECLASSIFICATION/DOWNGRADING SCHEDULE	
16. DISTRIBUTION STATEMENT (of this Report)  Approved for public release; distribution unlimited			
17. DISTRIBUTION STATEMENT (of the abstract entered in Block 20, if different from Report)  None			
18. SUPPLEMENTARY NOTES  None			
19. KEY WORDS (Continue on reverse side if necessary and identify by block number)  Raman Down Conversion, XeF Laser Injection Locking, Blue-Green Laser, Raman Oscillator-Amplifier Scheme			
20. ABSTRACT (Continue on reverse side if necessary and identify by block number)  Injection locking performance of a 1 $\mu$ s XeF laser pulse and Raman converter scaling have been investigated.  Narrowband ultraviolet radiation from a frequency-doubled dye laser has been used to control the linewidth and polarization of a long pulse-length electron beam-excited XeF laser. Linewidths of 0.004 nm have been achieved in the 353 nm band			

DD FORM 1 JAN 73 1473

EDITION OF 1 NOV 65 IS OBSOLETE  
S/N 0102-014-6601

SECURITY CLASSIFICATION OF THIS PAGE (When Data Entered)

of the XeF (B-X) Laser transition. Over 90% of the energy in the free-running laser pulse has been extracted in the narrowband injection-locked pulse. Ratios of injection signal power to output laser power on the order of  $10^{-5}$  are adequate for efficient injection-locking to occur.

Efficient Raman conversion of microsecond-pulse, injection-locked XeF (353 nm) laser radiation into the blue-green region via the second Stokes shift in hydrogen has been demonstrated using a Raman oscillator-amplifier scheme. Strong depletion of the pump and the first Stokes radiation accompanied by a dominant second Stokes (500 nm) output was observed for the first time. Amplifier power conversion efficiency of 43% was achieved along with a blue-green output energy of 1.7 J at an energy efficiency of 34%. These data support Raman converter scaling analyses which predict feasibility of efficient XeF-to-blue-green conversion at higher energies.

SCALING STUDIES OF EFFICIENT  
RAMAN CONVERTERS

Program Code No.: N00014

DARPA Order No.: NR395-706/DARPA Order  
No. 3125 AM #15

Contract Number: N00014-80-C-0442

Principal Investigator(s)  
and Telephone Number: Dr. H. Komine  
(213) 377-4811

Name of Contractor: Northrop Corporation  
Northrop Research and  
Technology Center

Effective Date of Contract: 21 March 1980 through  
20 March 1981

Amount of Contract: \$559,957

Sponsored by: DARPA  
1400 Wilson Blvd.  
Arlington, Virginia

Accession For	
NTIS GRA&I	<input checked="checked" type="checkbox"/>
DTIC TAB	<input type="checkbox"/>
Unannounced	<input type="checkbox"/>
Justification	
By _____	
Distribution/	
Availability Codes	
Dist	Avail and/or Special
<b>A</b>	
<b>DTIC</b> COPY INSPECTED 3	

## TABLE OF CONTENTS

	Page
1.0 INTRODUCTION	1
2.0 XeF LASER INJECTION LOCKING	3
2.1 Coaxial Laser Experiment	3
2.2 SWAT Laser Experiment	8
3.0 RAMAN CONVERSION	12
3.1 Scaling Analysis	12
3.2 Raman Oscillator-Amplifier Experiments	21
APPENDIX A	
APPENDIX B	

## LIST OF FIGURES

FIGURE	Page
1. Coaxial XeF Laser Injection Locking Experiment	3
2. Coaxial E-Beam XeF Laser Resonator	4
3. Injection Locked XeF Laser Spectrum	5
4. Injection Locked XeF Laser Spectrum	6
5. XeF Linewidth Measurement Laser Injection Locked at 353 nm	7
6. Injection Locking Temporal Character	7
7. SWAT XeF Laser Injection Locking Experimental Layout	8
8. Laser Pulse	9
9. Spectrograph Data of XeF 353 nm Band: Free-Running and Injection Locked Laser Spectra	11
10. Raman Oscillator Pump Energy and Cell Length vs Pulse Length	14
11. Saturation in Tightly Focused Oscillator	15
12. Pump Depletion in Optimized Oscillator	15
13. Second Stokes Power Conversion vs Raman Amplifier Gain for Various Stokes Injection Levels	17
14. Raman Amplifier Length vs Pulse Length for Various Stokes Injection Levels ( $T_i$ ) and Saturation Levels ( $\varphi$ )	18
15. Raman Amplifier Length vs $H_2$ Density	19
16. Conceptual Schematic of High Energy Raman Converter	20
17. AURORA System Experiment Layout	21
18. Amplifier Energy Conversion Efficiency for $S_1$ and $S_2$ Output at $H_2$ Pressures of 100 and 70 psig	23
19. XeF Laser Raman Conversion Amplifier Results	24



## 1.0 INTRODUCTION

An efficient blue-green laser source is being sought for a strategic submarine communication system as well as other applications. The rare-gas halide excimer lasers developed over the past few years appear to meet the requirement on efficiency and scalability, but the wavelength of their near-UV emission must be shifted into the blue-green spectral region. A novel conversion scheme for efficient wavelength shifting was conceived at Northrop Research and Technology Center in 1977. This concept, based on higher-Stokes-order Raman scattering in molecular gases, uses a Raman oscillator-amplifier combination to achieve optimized conversion into a particular Stokes order. Experimental feasibility of this concept was demonstrated under a Navy-sponsored program in 1979.

The initial experiments on the Raman oscillator-amplifier scheme used hydrogen gas as the Raman medium and a frequency-tripled Nd:YAG laser (355 nm) as an UV pump laser. Amplifier photon conversion efficiencies as high as 51 percent have been obtained for the second Stokes order (503 nm) output, in very good agreement with computer calculations. The laser pulse length in these experiments was relatively short (6 ns), which limits the amplifier energy conversion efficiency because of reduced Raman gain at the leading and trailing edges of the pulse. For longer, nearly rectangular pulses, and flat-topped beam profiles as obtained with large Fresnel number unstable resonators, conversion efficiencies approaching the quantum limit should be possible for second and third Stokes order converters.

In order to assess the scaling feasibility of this wavelength shifting technique for larger energies and longer pulse lengths, an analytical and experimental investigation was carried out, the results of which are discussed in this report. The objectives of the investigation were two-fold: First, to demonstrate narrow spectral bandwidth output with a 1  $\mu$ s XeF laser pulse via injection locking; second, to generate a Raman converter scaling model along with supporting experimental data.

The motivation for achieving a narrow-bandwidth XeF laser output was to meet the bandwidth requirement on the Raman-shifted blue-green output for communication applications. The Raman shifting experiment was aimed at demonstrating efficient XeF-to-blue-green conversion with up to 1  $\mu$ s pulse length and over a joule output.



The results of narrow bandwidth XeF laser injection locking experiments and Raman conversion scaling studies are described in sections 2 and 3, respectively.

## 2.0 XeF LASER INJECTION LOCKING

The feasibility of efficient injection locking at spectral bandwidths much narrower than the free-running XeF laser spectrum was demonstrated with a small e-beam pumped XeF laser. Scaling to a larger volume, long-pulse XeF laser was also accomplished. The injection source of these experiments was obtained from a tunable narrow-bandwidth frequency-doubled pulsed dye laser system. The details of the experimental setup and the results are presented in the following sections.

### 2.1 Coaxial Laser Experiment

Initial investigation of XeF laser injection locking was performed with a coaxial e-beam excited device. A combination of injection-locked dye laser system followed by a frequency doubler generated a tunable narrow band ( $\Delta\nu \sim 0.3 \text{ cm}^{-1}$ ) UV source near 353 nm, as schematically shown in Figure 1.

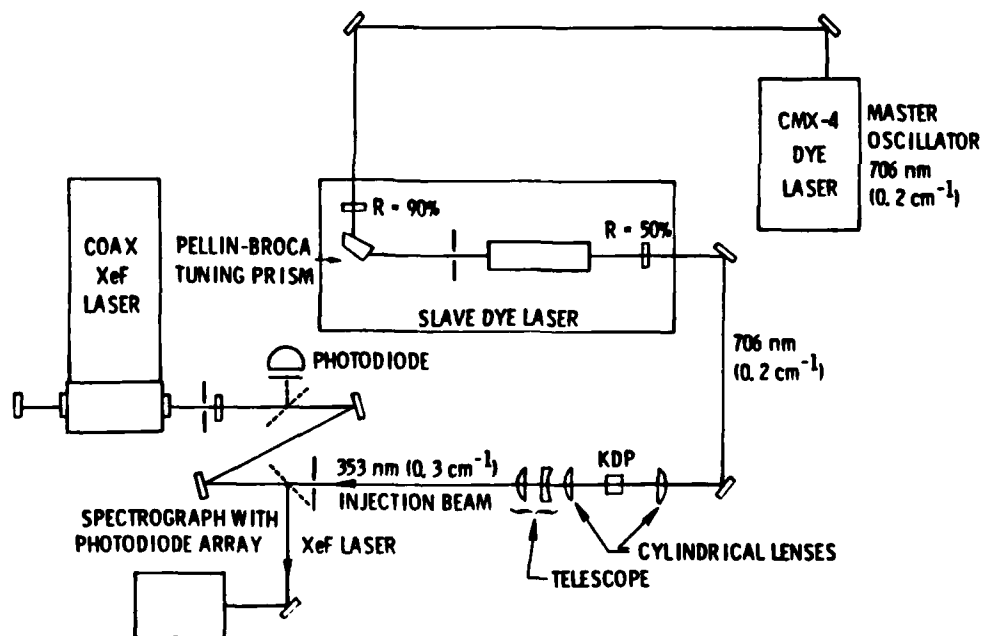


FIGURE 1. COAXIAL XeF LASER INJECTION LOCKING EXPERIMENT

The XeF laser was operated at room temperature with a gas mixture of  $\text{NF}_3$  (0.12%), Xe (0.5%), and balance Ne at a total pressure of 3 atm. The laser cavity is schematically shown in Figure 2. The gain medium is contained in a cylinder

2.3 cm in diameter, 25 cm long, with 0.025 mm-thick titanium foil walls. This cylinder also serves as the anode for a coaxial electron beam used to excite the gases. The electron beam is driven by a 3-stage Marx bank, when charged to 90 kV per stage, produces current densities through the anode foil walls on the order of  $8 \text{ A/cm}^2$ . The optical elements in the cavity are two anti-reflection coated  $\text{CaF}_2$  windows and flat dielectric mirrors with  $R = 99\%$  and  $65\%$  at 353 nm.

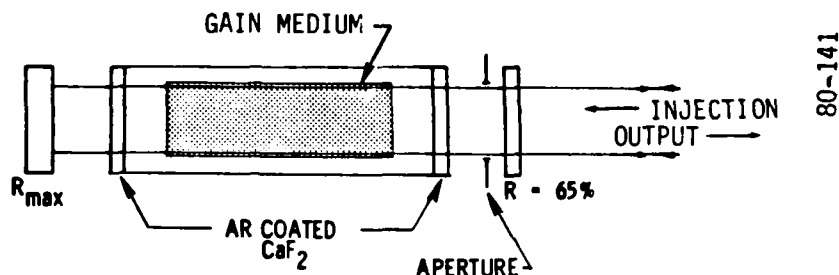
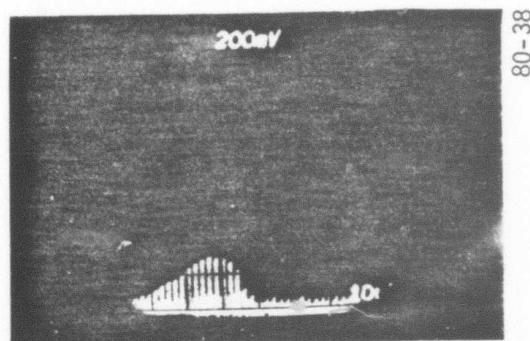


FIGURE 2. COAXIAL E-BEAM XeF LASER RESONATOR

A spectrograph with a linear photodiode array located at the film plane was used to monitor the free-running and injection locked XeF laser output. Typical data are shown in Figure 3(a) and (b). Vertical "spikes" make up a light intensity profile sampled by the individual photodiodes of the array. Figure 4 shows a comparison of unlocked and locked spectra along with an overlap indicating the actual bandwidth determined by a Fabry-Perot interferometer. Figure 5 shows a typical locked spectrum obtained by a Fabry-Perot interferometer with a free spectral range of  $1.7 \text{ cm}^{-1}$ . Based on these data, the locked spectral bandwidth is  $\Delta\nu \approx 0.3 \text{ cm}^{-1}$  or  $\Delta\lambda \approx 0.004 \text{ nm}$  at  $\lambda = 353 \text{ nm}$ .

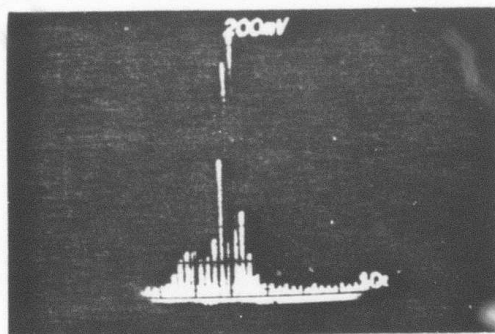
The XeF laser produced an output of 80 mJ in 140 ns, yielding a peak power of 0.57 MW under free-running conditions. To lock this laser, injected energy of  $60 \mu\text{J}$  inside the resonator in a 500 ns pulse was found to be adequate to extract  $> 90\%$  of the free-running laser output in a narrow band. A typical temporal pulse overlap of the laser and the injection radiation is shown in Figure 6. These measurements indicate a ratio of XeF output power to the injection power in excess of 5000.

In conclusion, the coaxial laser experiments demonstrated the feasibility to lock an e-beam excited XeF laser to a spectral bandwidth of  $0.3 \text{ cm}^{-1}$  at an



(1.25 Å/DIV)

(a) XeF LASER 353 nm BAND SPECTRUM



(b) INJECTION-LOCKED XeF LASER SPECTRUM  
(INSTRUMENT LIMITED RESOLUTION  $\approx .4$  Å FWHM)

FIGURE 3. INJECTION LOCKED XeF LASER SPECTRUM

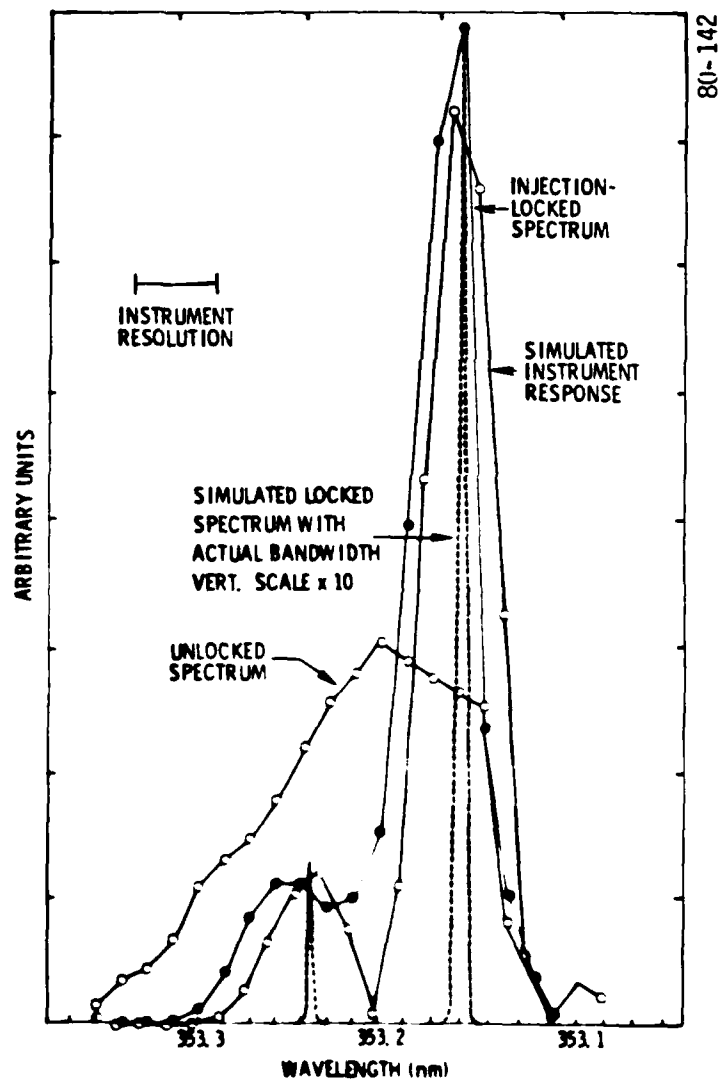
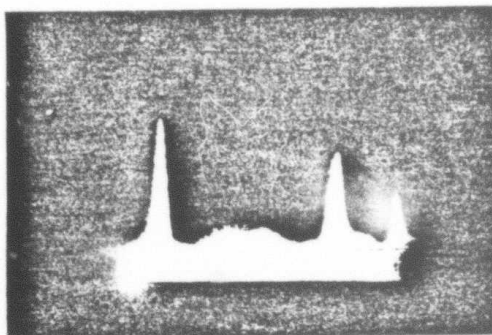


FIGURE 4. INJECTION LOCKED XeF LASER SPECTRUM



LINEWIDTH MEASURED USING A SOLID FUSED SILICA ETALON  
 (FREE SPECTRAL RANGE =  $1.7 \text{ cm}^{-1}$ )  
 $\Delta\nu \approx 0.3 \text{ cm}^{-1}$  ( $\Delta\lambda \approx 0.004 \text{ nm}$ )

FIGURE 5. XeF LINEWIDTH MEASUREMENT LASER INJECTION  
 LOCKED AT 353 nm

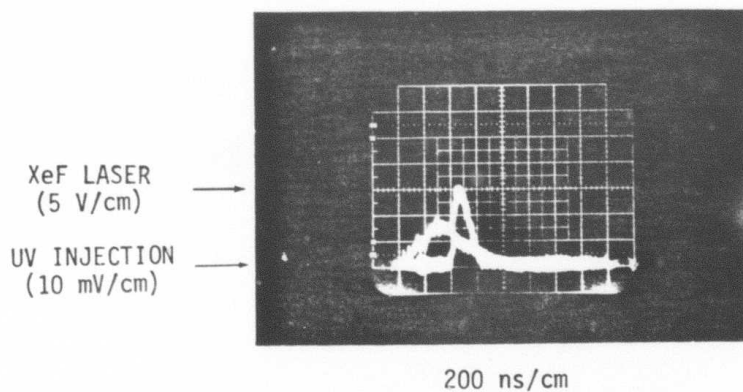


FIGURE 6. INJECTION LOCKING TEMPORAL CHARACTER

injection level of  $\leq 2 \times 10^{-4}$  relative to the laser power. This is an improvement of a factor of 4 in bandwidth reduction relative to earlier work on XeF injection locking [GDB77]. Further discussion of the present experiment is given in Appendix A.

## 2.2 SWAT Laser Experiment

Scaling of XeF laser injection locking to larger energies and longer pulses was conducted with a 10-eV e-beam excited device (SWAT). Experimental arrangement, shown in Figure 7, included the injection source and diagnostics similar to those used in the initial experiments with the coaxial laser.

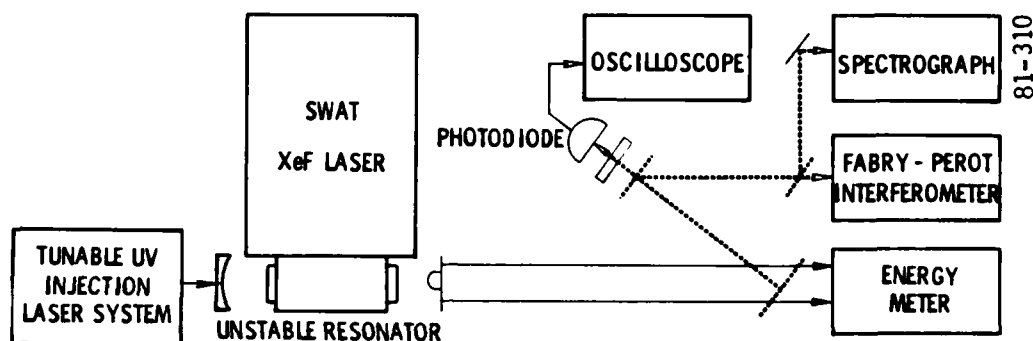
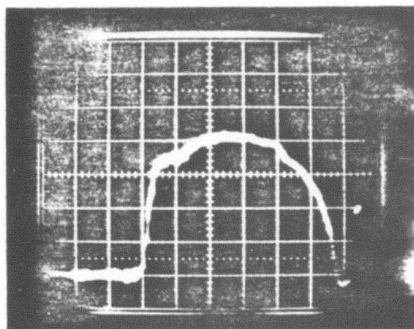


FIGURE 7. SWAT XeF LASER INJECTION LOCKING EXPERIMENTAL LAYOUT

The SWAT laser employed a positive-branch confocal unstable resonator of magnification 2.2. The primary concave reflector ( $R = 10$  m) had a 3 mm diameter hole at the center for coupling the injection radiation. A 5 cm diameter convex reflector ( $R = 4.5$  m), mounted on a 4-vane "spider", formed the output coupler.

The SWAT device operated with a 3-stage Marx bank which, when charged to 120 kV per stage, produced  $\geq 10$  A/cm<sup>2</sup> current density through 0.05 mm-thick aluminum foil. The excited gas region is approximately 10 cm x 10 cm cross section by 100 cm long. A pair of coils around the plenum provided a magnetic guide field to improve the uniformity of energy deposition. Maximum output from the device was  $\sim 10$  J in a  $\sim 1$   $\mu$ s long optical pulse at 353 nm. No lasing action at 351 nm was observed. A representative oscillogram of free-running laser pulse is shown in Figure 8.





200 ns/DIV.

$E = 8.7 \text{ J}$

1.8 Torr  $\text{NF}_3$  (0.1%)

5.5 Torr Xe (0.3%)

37 psi Ne

360 kV

FIGURE 8. LASER PULSE

Injection locking of the SWAT laser was achieved with an injection power level of about 200 W. The locked XeF output power was approximately 8 MW, which yields an injection level to laser output power ratio of  $2.5 \times 10^{-5}$ . The measured bandwidth of the locked spectrum was approximately  $0.5 \text{ cm}^{-1}$  ( $\Delta\lambda \approx 0.006 \text{ nm}$ ) at 353 nm, when the injection wavelength was tuned to the peak of the XeF emission band. Figure 9 shows typical spectrograph data of the free-running and injection locked XeF output.

The laser output increased slightly with injection locking, which was attributed to an onset of laser oscillation occurring 100 to 200 ns earlier than the free-running case. This onset of laser oscillation was dependent on the detuning of the injection wavelength relative to the peak of the free-running spectrum. The risetime of the onset was fastest with zero detuning (to the extent of  $\pm 1$  photodiode response of the spectrograph:  $\Delta\lambda \approx 0.025 \text{ nm}$ ). A non-zero detuning resulted in a slower risetime. Detuning to the longer wavelength side resulted in incomplete locking of the output into the injection spectrum bandwidth; a residual lasing was observed at the peak of the 353 nm band. Injection locking was not possible when the detuning was to the shorter wavelength side.

These data indicate that XeF 353 nm band can be efficiently locked to a narrow bandwidth injection source under long pulse excitation ( $\sim 1 \mu\text{s}$ ) with  $\sim 10 \text{ J}$  output. The measured spectral bandwidth of  $0.5 \text{ cm}^{-1}$  is close to the eventual transmitter requirement of the blue-green laser communication. However, it is important to note that injection locking efficiency is reduced significantly when the injection wavelength is detuned from the peak of the free-running laser spectrum.

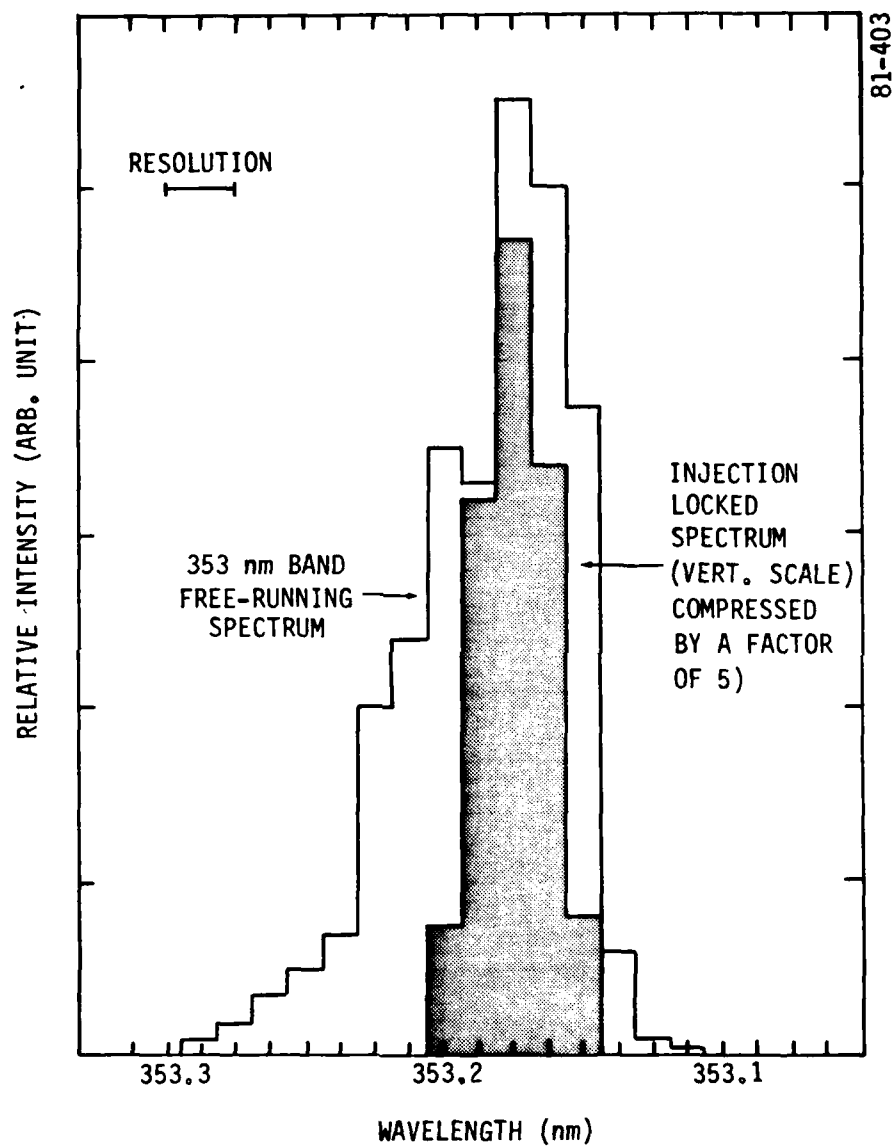


FIGURE 9. SPECTROGRAPH DATA OF XeF 353 nm BAND:  
FREE-RUNNING AND INJECTION LOCKED LASER SPECTRA

### 3.0 RAMAN CONVERSION

Investigation of Raman converter scaling was carried out in two parts. The first part was the scaling analysis of converter systems based on oscillator-amplifier combination scheme. In the second part experiments were conducted to test an oscillator-amplifier with  $1\text{ }\mu\text{s}$  pump pulses using the SWAT XeF laser. Key findings of the two parts are discussed in the following sections.

#### 3.1 Scaling Analysis

Analysis of Raman converter systems based on oscillator-amplifier concept has been carried out in terms of optimum design within the frame-work of material and Raman medium constraints. Key results of this analysis include energy limitation of an optimized oscillator, amplifier system configuration versus energy scaling, and identification of critical technology issues relevant to converter systems design. Details of these findings are described below:

- Raman Oscillator

The purpose of an oscillator is to generate nearly diffraction limited multiple-order Stokes beams with high efficiency. The Stokes pulse length should be as close to the pump pulse length as possible in order to provide injection signal to an amplifier over most of the amplifier pump pulse. A single-pass super-fluorescent oscillator can meet these requirements under proper conditions of pump energy and focusing geometry.

The basic constraint imposed on the oscillator design is saturation of the Raman medium. The volume of hydrogen gas accessible to Raman scattering is defined by a diffraction limited focal area and an effective interaction length given by the confocal parameter of the focused pump beam. Experiments [KS79] have shown that such a focused pumping geometry can generate nearly diffraction limited Stokes beams in agreement with theoretical model calculations. Since a hydrogen molecule is excited into the first vibrational level for each pump laser photon scattered into Stokes radiation, the ground state population is continually depleted during Raman conversion process until gain is saturated (thereby terminating the process). If the saturation level,  $\varphi$ , is defined as a fraction of molecules transferred out of the ground state, then confocal parameter,  $b$ , is given by

$$b \approx \left[ \frac{mG_o \lambda \tau}{\varphi N g h c} \right]^{1/2}$$

where  $N$  = hydrogen number density,  $g$  = gain coefficient,  $G_o$  = oscillator threshold gain,  $m$  = number of times above threshold,  $\lambda$  = pump wavelength, and  $\tau$  = pulse length.

This requirement implies a certain cell length so that the pump beam fluence on the windows is below the damage limit. Using gaussian beam propagation relations, the necessary cell length,  $l$ , is found to be

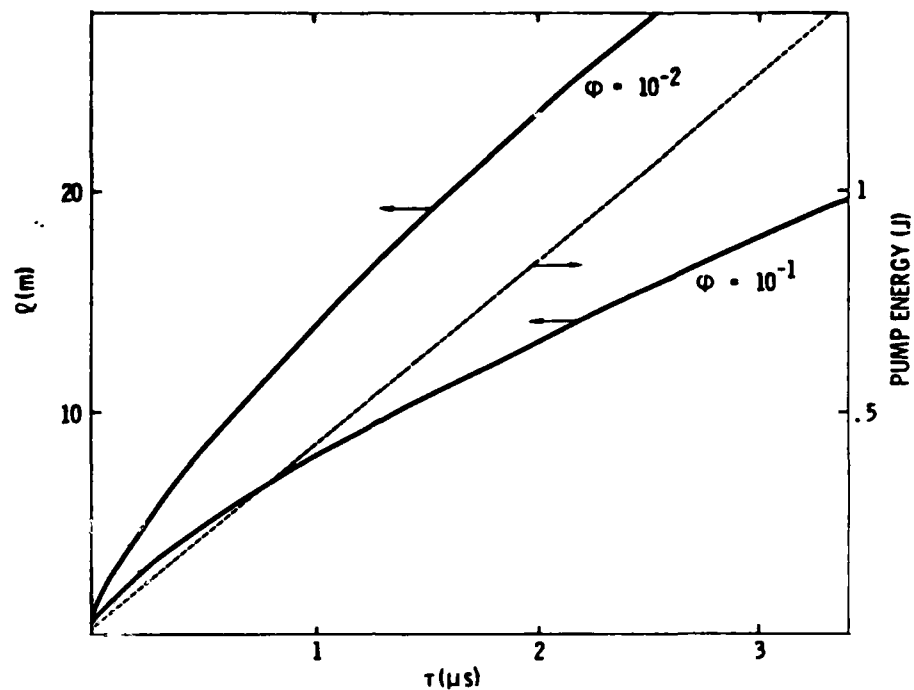
$$l \approx \left[ \frac{2mG_o b \tau}{9F_o} \right]^{1/2}$$

where  $F_o$  is the oscillator window fluence. These expressions can be combined to yield pump energy requirement assuming a diffraction limited beam. The result is given by

$$E_o \approx \frac{mG_o \lambda \tau}{2g} .$$

This states that pump energy consistent with saturation and optical damage constraints is limited to a certain value essentially determined by the pulse length. The other parameters are restricted by the physics of Raman conversion. For example, the value of  $m$  should be 3 to 4 for optimum first and second Stokes output, and  $G_o$  is assumed to be about 30. For XeF laser pulse of 1  $\mu$ s, the pump energy is approximately 0.5 J. Much lower energies will not generate Stokes output, while much higher energies will cause window damage or saturation problems.

The relations discussed above are graphically illustrated in Figure 10, in which the cell length is plotted as a function of pulse length for two values of saturation at 6 amagats of  $H_2$  gas. The pump energy requirement is also shown as a function of pulse length. For these curves a fluence value of 5 J-cm<sup>-2</sup> was used.



81-45

FIGURE 10. RAMAN OSCILLATOR PUMP ENERGY AND CELL LENGTH VS PULSE LENGTH

To verify some of these calculations, two focusing geometries were tested: tight-focusing and optimized configuration. Figure 11 shows pump and Stokes pulse shapes for the tight-focusing case. It is clear that short Stokes pulses are caused by saturation of the medium which is indicated by a partial pump depletion at the beginning of the pump pulse. Figure 12 shows the results of an optimized case. Stokes pulses are efficiently generated over the entire pump pulse duration accompanied by a uniform pump depletion of about 60%. This value is consistent with the calculated energy content of the central lobe of our focused unstable resonator mode.

#### • Raman Amplifier

Our basic oscillator-amplifier scheme utilizes a collimated beam geometry in a single amplifier to convert pump radiation into the second Stokes output. This is accomplished by injecting a low level of well-controlled first and second Stokes beams into an amplifier whose length is given by

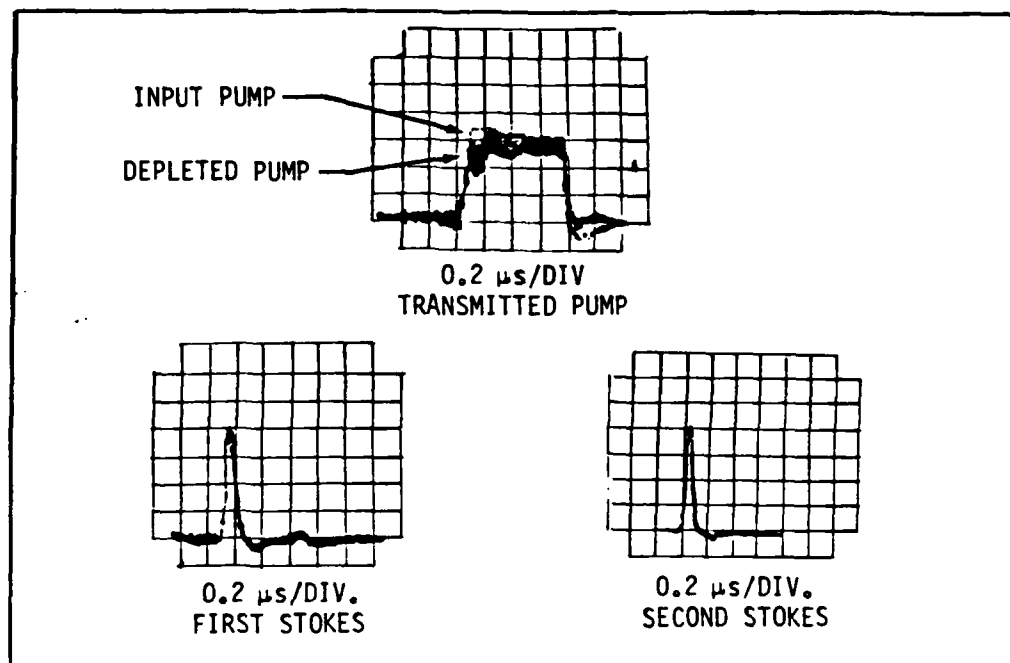


FIGURE 11. SATURATION IN TIGHTLY FOCUSED OSCILLATOR

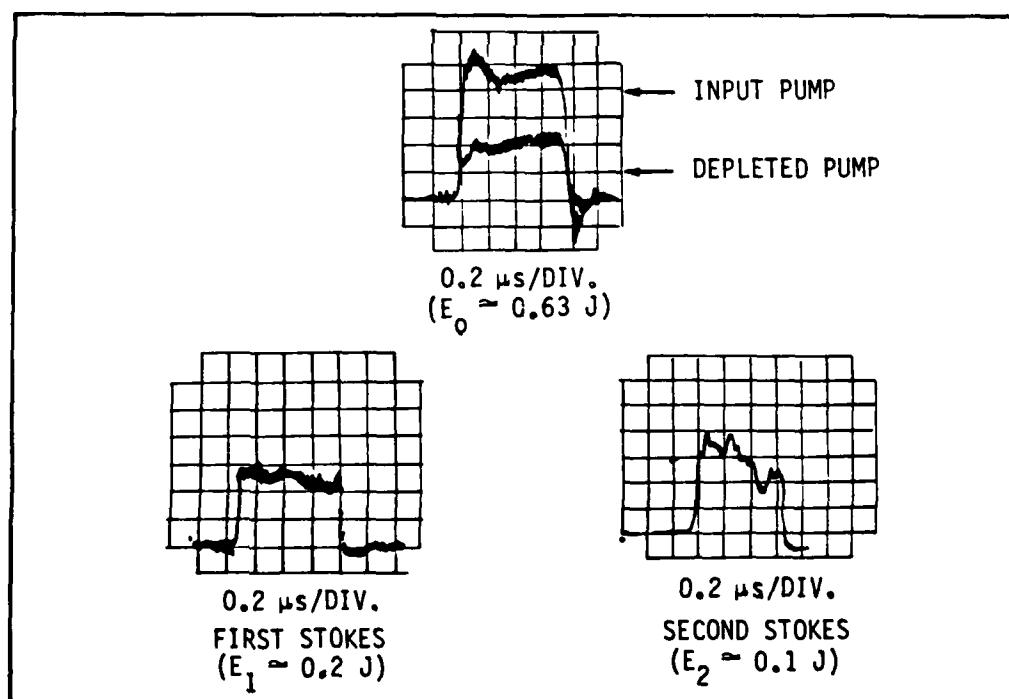


FIGURE 12. PUMP DEPLETION IN OPTIMIZED OSCILLATOR



$$L = \frac{G\tau}{gF}$$

where

G = amplifier gain

$\tau$  = pulse length

g = gain coefficient

F = amplifier window fluence

This relationship applies to the case of long pulse pump laser where fluence rather than intensity determines optical damage limitation on the Raman cell window. In the case of an e-beam pumped XeF laser with  $\tau \sim 1 \mu s$ , the amplifier length is determined by a proper choice of G, g, and F. These parameters, in turn, depend on specific design constraints of a given converter. A procedure for selecting optimum parameters has been developed and is discussed below.

The choice of G is dependent on the level of Stokes injection. Loosely speaking, the higher the injection level, the smaller the gain can be to achieve efficient conversion. To investigate the range of optimum G values, an amplifier simulation code was used to calculate second Stokes power conversion versus G for various injection levels denoted by  $\eta$ . The results are shown in Figure 13. The value of  $\eta$  for the first and second Stokes are assumed to be equal while the third Stokes level is taken to be 3 orders of magnitude smaller. It is apparent that a wide range of G yields efficiencies close to the quantum limit under ideal conditions. However, in a real amplifier, there may be parasitic oscillations if the gain is excessively high. To avoid this potential problem, the gain should be below 30. This implies that injection levels should be at least  $10^{-4}$ . From practical consideration  $\eta \geq 10^{-3}$  is more attractive since substantial spatial and temporal intensity (gain) variations can be tolerated without reduction in efficiency. It is significant to note that these considerations roughly define a scaling factor for amplifier system configuration. This point will be discussed in more detail later.

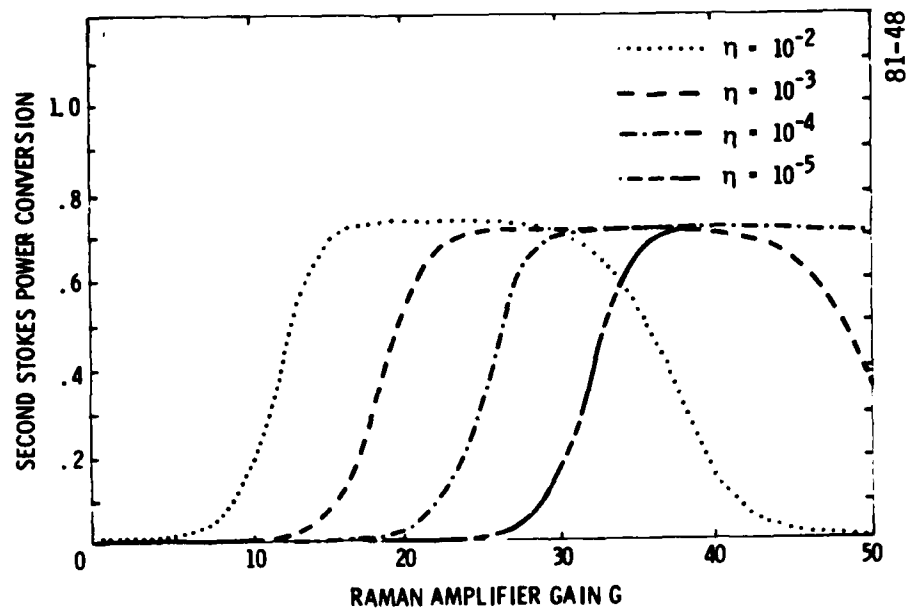


FIGURE 13. SECOND STOKES POWER CONVERSION VS RAMAN AMPLIFIER GAIN FOR VARIOUS STOKES INJECTION LEVELS

Based on the above results, one can calculate minimum amplifier length versus pulse length. Figure 14 shows such a calculation for the case of four amagats of hydrogen gas and  $5 \text{ J-cm}^{-2}$  fluence. It indicates that a 10 m amplifier with  $\eta = 10^{-3}$  is required for a  $1 \mu\text{s}$  pulse. Also shown in this figure is a length requirement imposed by medium saturation,  $\phi$ . Two sets of curves for  $\phi = 10^{-4}$  and  $\phi = 10^{-3}$  show that for  $\tau \geq 1 \mu\text{s}$ , the amplifier length requirement due to optimum gain is more important. Thus, medium saturation may be considered to be negligible under optimum conditions.

Amplifier length is also dependent on hydrogen number density,  $N$ , through gain coefficient dependence on  $N$ . Because of the form of Raman linewidth as a function of density, the gain coefficient varies according to

$$g = \frac{\bar{g}}{1 + (N_c/N)^2}$$

where

$\bar{g}$  = high density limit of gain coefficient

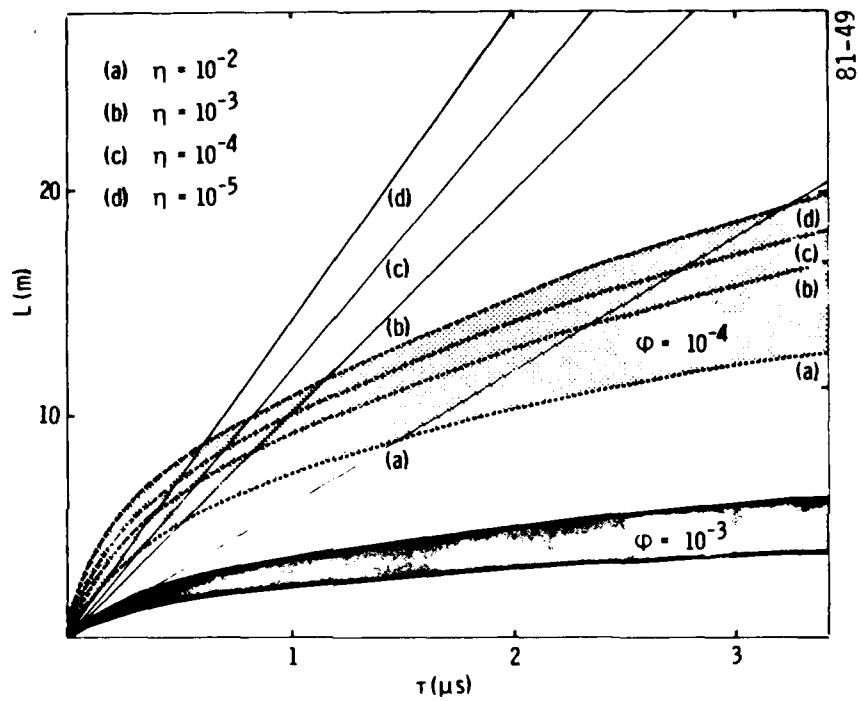


FIGURE 14. RAMAN AMPLIFIER LENGTH VS PULSE LENGTH  
FOR VARIOUS STOKES INJECTION LEVELS ( $\eta$ ) AND  
SATURATION LEVELS ( $\phi$ )

$N_c$  = density where Raman linewidth  
is a minimum

This relation can be used to derive length scaling by hydrogen number density. Since the minimum linewidth occurs near 2.4 amagats [Ow79], a significant reduction in length can be realized by increasing  $N$  from 4 to 8 amagats, as illustrated in Figure 15.

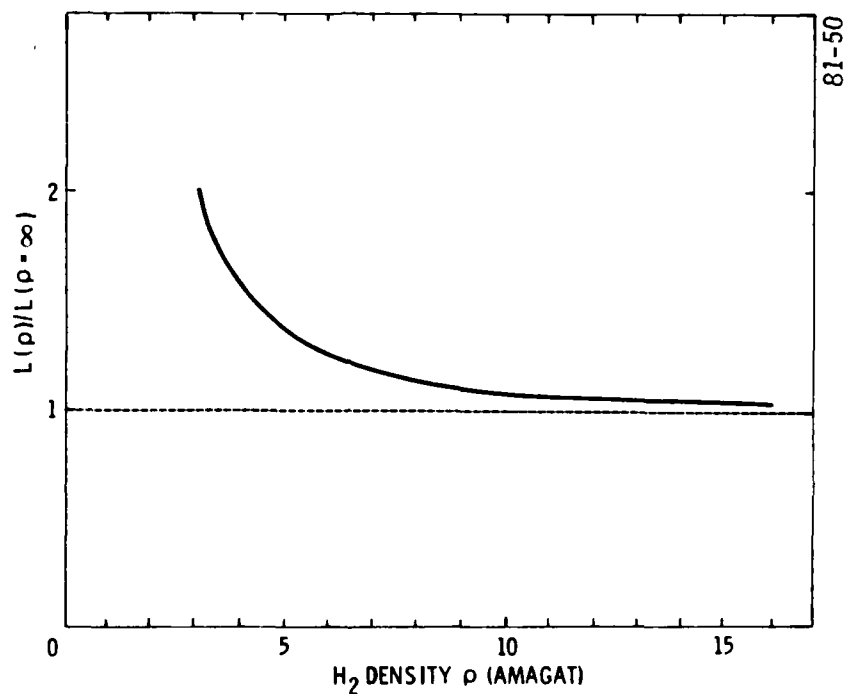


FIGURE 15. RAMAN AMPLIFIER LENGTH VS  $H_2$  DENSITY

The fluence plays an important role in defining the size of Raman amplifier. Fluence not only determines  $L$  but also beam size,  $s$ , according to

$$s = \sqrt{E/F} .$$

For example, a 5 J pump laser requires  $s = 1$  cm if  $F = 5 \text{ J} \cdot \text{cm}^{-2}$  is used. On the other hand, if  $E = 500 \text{ J}$ , the aperture size increases to 10 cm. This clearly shows the desirability of increased values of fluence. Even a two fold increase in  $F$  can reduce the cell length in half and the aperture size by

$1/\sqrt{2}$ . In general, the volume of Raman amplifier is inversely proportional to the square of the fluence. Therefore, further advances in higher damage threshold windows and mirrors will have a significant technological impact on converter design and engineering.

- Converter System Configuration

The foregoing sections described design parameters for optimized oscillator and amplifier stages. For the oscillator, we found an energy limitation of about 0.5 J (TEM<sub>00</sub> pumping) for a 1  $\mu$ s pulse. Based on oscillator experiments, Stokes output near 0.1 to 0.2 J should be possible. Using these as injection into an amplifier of  $\eta < 10^{-3}$ , pump energy for the amplifier may be on the order of 100 J. This implies that a single amplifier stage may be limited to several hundred joules level pump laser because of practical considerations on efficiency and well-controlled output beam. Therefore, for higher energy lasers, one must devise a method to inject Stokes energies of at least  $10^{-3}$  times the pump energy.

A logical solution to this scale factor limitation due to  $\eta$  is an extension of the oscillator-amplifier concept to include a preamplifier stage. The purpose of a preamplifier is to boost first and second Stokes outputs of an oscillator to a level sufficient for a final amplifier stage. Since the injection input into the final amplifier must consist of both first and second Stokes, the preamplifier must be optimized to generate both Stokes efficiently. This means that the gain in the preamplifier should be selected such that power conversion curves for two Stokes have similar values. A conceptual schematic of an oscillator-preamplifier-amplifier system is illustrated in Figure 16.

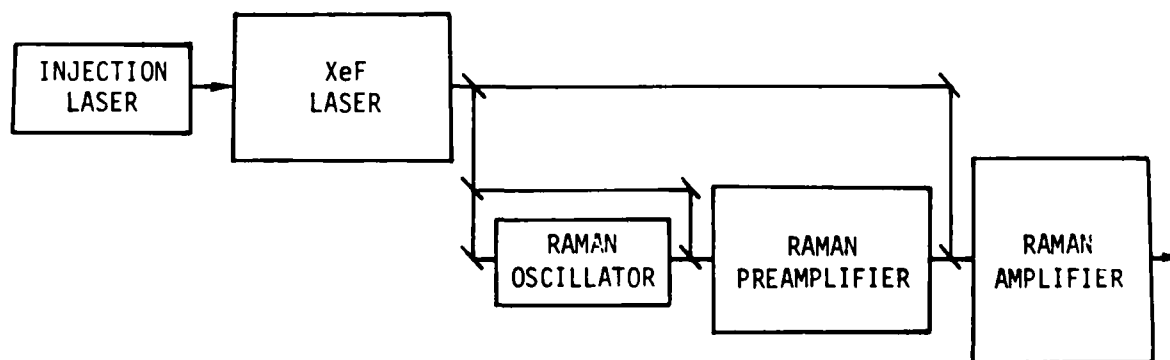


FIGURE 16. CONCEPTUAL SCHEMATIC OF HIGH ENERGY RAMAN CONVERTER

### 3.2 Raman Oscillator-Amplifier Experiments

Previous experiments on higher-Stokes-order Raman oscillator-amplifier combination schemes demonstrated high conversion efficiencies of shifting UV radiation into the blue-green region [KS79][KS80]. These experiments were conducted with relatively low energies ( $< 20$  mJ) and short optical pump pulse ( $\leq 10$  ns). In order to extend the data base to higher energies and longer pulse lengths up to  $1 \mu\text{s}$ , the XeF laser output of the SWAT device was used. Injection locking was used throughout the Raman conversion experiments to achieve a narrow bandwidth pump source. This permitted the use of gain-enhancement technique [SLK80] to optimize Raman gain.

A schematic of the experimental facility including the SWAT laser and the AURORA (Advanced UV-Pumped Raman Oscillator-Raman Amplifier) system is shown in Figure 17. The oscillator was a 2 m long cell filled with 100 to 120 psig of research grade hydrogen gas. When pumped with 0.63 J of input energy after a beam splitter (BS) this oscillator produced superfluorescent output at 414 nm (first Stokes =  $S_1$ ), 500 nm (second Stokes =  $S_2$ ), and 631 nm (third Stokes =  $S_3$ ). The pulse shape and energy output data (discussed in 3.1) indicated efficient oscillator conversion into  $S_1$  and  $S_2$ .

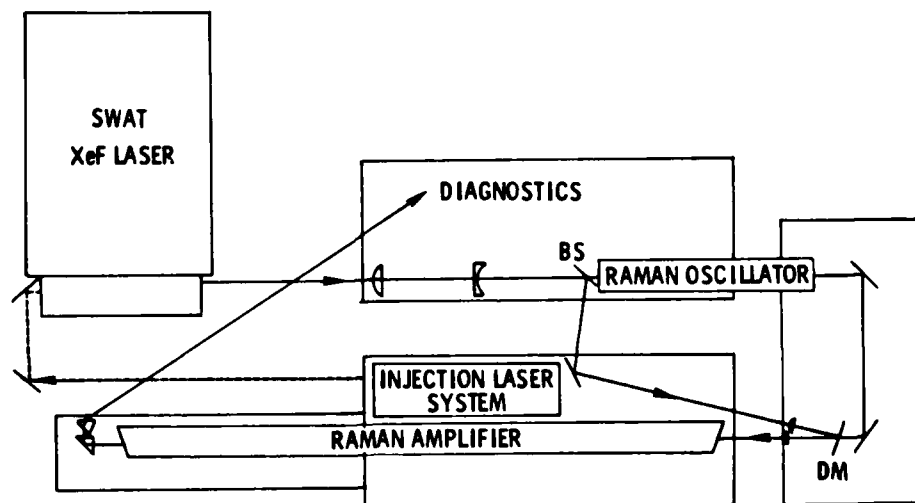


FIGURE 17. AURORA SYSTEM EXPERIMENT LAYOUT

81-303

The  $S_1$  and  $S_2$  beams from the oscillator provided the Stokes injection radiation into an amplifier. These beams were spatially and temporally matched to the amplifier pump beam before being combined and overlapped at a dichroic mirror (DM).

The amplifier cell was 6 m long and filled with up to 100 psig of research grade hydrogen gas. Clear apertures of 3 cm diameter at each end permitted adequate clearance of the 1 cm diameter pump and Stokes beams. Further details are described in Appendix B.

Parametric measurements of amplifier performance included energy conversion efficiencies for  $S_1$  and  $S_2$  as a function of amplifier pump energy at different  $H_2$  pressures. Figure 18 shows the data taken at  $H_2$  pressures of 100 psig and 70 psig. The maximum  $S_2$  energy output of 1.7 J (corrected for output window transmission) was obtained at  $E_p \approx 5.1$  J with  $p = 100$  psig, yielding 34% blue-green energy efficiency in the amplifier. The  $S_1$  efficiency for the same conditions was 24%, indicating that the dominant output was  $S_2$  for the first time. At 70 psig pressure, the  $S_1$  efficiency was higher than that of  $S_2$ . However, the variation with pump energy clearly indicates that  $S_2$  efficiency can be expected to surpass the  $S_1$  value at higher pump energies (see dashed lines in Figure 18). This behavior is expected since higher pump intensities are needed to compensate for gain coefficient reduction at lower pressures.

The temporal conversion data showed strong pump depletion and a varying degree of  $S_1$  depletion and  $S_2$  amplification. A set of oscillograms for the data corresponding to the maximum  $S_2$  output is shown in Figure 19. The depleted pump,  $S_1$ , and  $S_2$  pulses were recorded simultaneously while the undepleted pump was taken without  $H_2$  gas. The undepleted and depleted pump traces are taken with the same photodiode and vertical scale, but 5.1 J refers to the amplifier input pump energy corresponding to the maximum  $S_2$  data. Hence, the pump depletion is measured to be  $(5.1 \text{ J} - 1.2 \text{ J})/5.1 \text{ J} = 76\%$ . It is significant to note that  $S_1$  pulse also shows strong depletion as indicated by a flat-top shape. This explains the observed high  $S_2$  conversion efficiency.

The  $S_2$  pulse shape resembles the undepleted pump pulse (except for the leading edge where gain is lower) which indicates that peak power conversion into  $S_2$  is



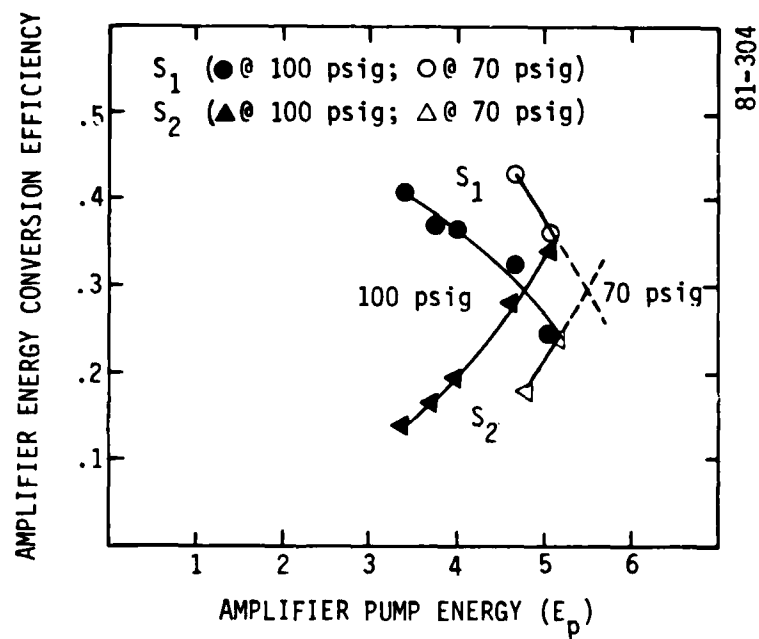


FIGURE 18. AMPLIFIER ENERGY CONVERSION EFFICIENCY FOR  $S_1$  AND  $S_2$  OUTPUT AT  $H_2$  PRESSURES OF 100 AND 70 psig

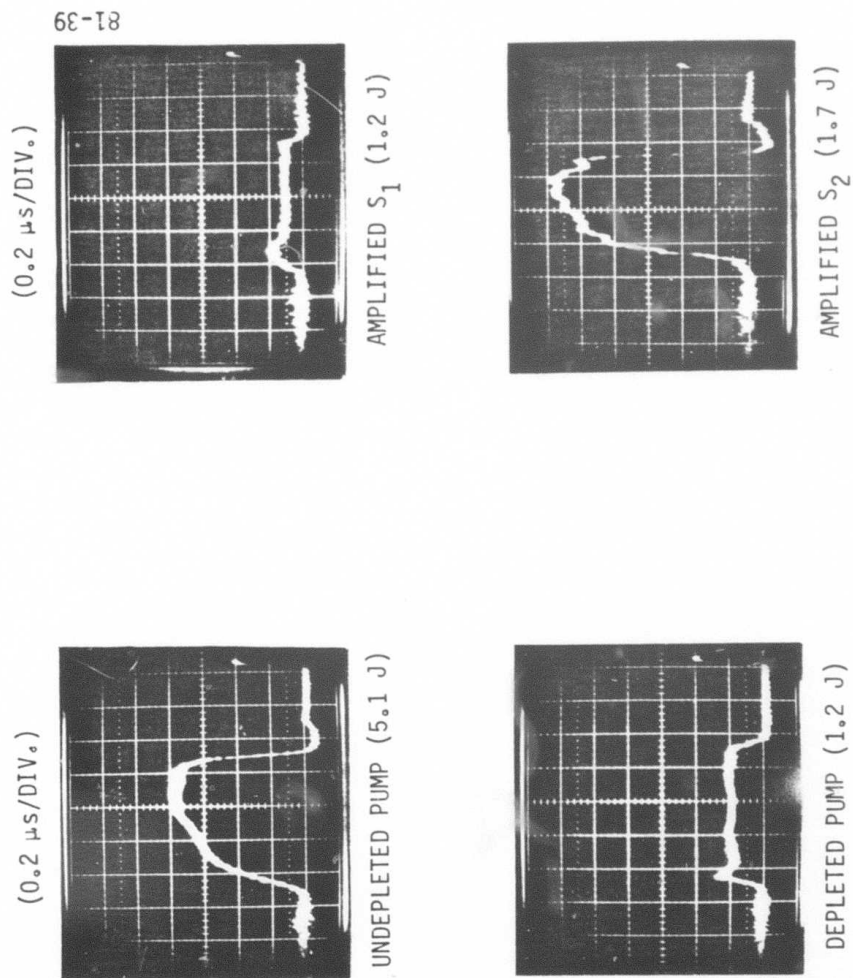


FIGURE 19. XeF LASER RAMAN CONVERSION AMPLIFIER RESULTS

approximately 43% (61% photon efficiency). Therefore, the data demonstrates, for the first time, that a Raman converter can be operated with a dominant higher Stokes order which can be selectively optimized with proper Stokes injection and amplifier gain.

In the present series of experiments, various factors were not optimized. For example, the XeF laser beam quality could be improved along with optical quality of the lenses and mirrors used in the setup. The unpolarized XeF output also reduced effective gain as well as pump and Stokes transmission through various optics. In spite of these shortcomings, the overall system efficiency, defined as the blue-green energy output divided by the XeF laser output, was 21%. Improvements in optical quality, polarization control, and beam quality are expected to provide an overall system efficiency greater than 30%.

In conclusion, the oscillator-amplifier Raman conversion experiments have verified the basic scaling feasibility of long pulse ( $\sim 1 \mu\text{s}$ ) conversion at a blue-green energy level in excess of 1 J. These results support the scaling analysis, and the prospects of scaling to higher energies appear to be encouraging.

## REFERENCES

- [GDB77] J. Goldhar, J. Dickie, L. P. Bradley, and L. D. Pleasance, Appl. Phys. Lett. 31, 677 (1977)
- [KS79] H. Komine and E. A. Stappaerts, Opt. Lett. 4, 398 (1979)
- [KS80] H. Komine and E. A. Stappaerts, Paper EE-8, International Lasers '80 Conference Proceedings (December 15 - 19, 1980)
- [Ow79] A. Owyong, Opt. Lett. 2, 91 (1978)
- [SLK80] E. A. Stappaerts, W. H. Long, Jr., H. Komine, Opt. Lett. 5, 4 (1980)

## APPENDIX A

### EFFICIENT INJECTION-LOCKING OF AN E-BEAM EXCITED XeF LASER<sup>†</sup>

John B. West, Hiroshi Komine,  
and Eddy A. Stappaerts

Northrop Corporation  
Northrop Research and Technology Center  
One Research Park  
Palos Verdes Peninsula, CA 90274

#### ABSTRACT

Narrowband ultraviolet radiation from a frequency doubled dye laser has been used to control the linewidth and polarization of a long pulse length electron beam-excited XeF laser. Linewidths of 0.004 nm have been achieved in the 353 nm band of the XeF B-X Laser transition. Over 90% of the energy in the free-running laser pulse has been extracted in the narrowband injection locked pulse. Ratios of injection signal power to output laser power on the order of 1:5000 are adequate for efficient injection-locking to occur.

---

<sup>†</sup>Research supported by Defense Advance Research Projects Agency under Contract N00014-80-C-0442

EFFICIENT INJECTION LOCKING OF  
AN E-BEAM EXCITED XeF LASER

John B. West, Hiroshi Komine,  
and Eddy A. Stappaerts

The XeF laser has been demonstrated to be an efficient source of near ultraviolet radiation.<sup>1,2</sup> However, many applications for this laser require a spectral linewidth which is considerably narrower than that obtained from a free-running device. The use of diffraction gratings and intracavity etalons to control the linewidth of a high energy device would not be practical because of optical damage problems. Thus, injection locking<sup>3</sup> is examined here as an alternative method. Goldhar et al<sup>4</sup> reported injection locking a short pulse length, e-beam excited XeF laser to a linewidth of 0.02 nm. We have applied this technique to electron beam excited XeF lasers having longer pulse lengths. Our results show that it is possible to injection lock a long pulse XeF laser to linewidths on the order of 0.005 nm with efficiencies on the order of 90%.

Figure 1 shows the experimental arrangement used in these studies. The XeF laser used in these experiments has been described elsewhere,<sup>5</sup> so only a brief description is given here. The laser gas, consisting of  $\text{NF}_3$ , Xe, and Ne with concentrations of 0.12%, 0.5%, and 99.38% at a total pressure of 3 atmospheres, is contained in a cylinder 2.3 cm in diameter, 25 cm long, with 0.025 mm thick titanium foil walls. This cylinder also serves as the anode for

a coaxial electron beam used to excite the gases. The electron beam is driven by a 3-stage Marx bank which, when charged to 90 kV per stage, produces current densities through the anode foil walls on the order of  $8 \text{ amps/cm}^2$ . Two flat dielectric mirrors with reflectivities of 99.9% and 65% at 353 nm comprise the optical resonator.

Under these conditions, the XeF laser output is typically 75 mJ in a 140 ns optical pulse. Laser energies are measured with a Gentec joulemeter, and temporal pulse shapes are observed using a vacuum planar photodiode (ITT F-4000 with S-5 photocathode). Spectra of the XeF laser output were recorded by dispersing the radiation with a 1 meter spectrometer onto a linear photodiode array (EGG Reticon RL256G). This allowed simultaneous observation of both the 353 and 351 nm bands of the XeF B $\rightarrow$ X transition. The spectrometer/diode array combination had a resolution limit of 0.04 nm. To observe a linewidth less than this, a Fabry-Perot etalon with a free spectral range of  $1.7 \text{ cm}^{-1}$  was used in conjunction with a second photodiode array to measure actual laser linewidths.

Narrow bandwidth ultraviolet radiation at 353 nm is produced by frequency doubling the output of an injection-locked, pulsed dye laser system. A Chromatix CMX-4 laser, with an intracavity etalon (free spectral range =  $6 \text{ cm}^{-1}$ ), is used as a master oscillator to produce narrow bandwidth radiation at 706 nm. A mixture of oxazine 720 ( $7.5 \times 10^{-5} \text{ M}$ ) and rhodamine 590 ( $1.2 \times 10^{-4} \text{ M}$ ) in



methanol was used in this laser. The output of this laser was injected into a Candela SLL625A coaxial flash lamp dye laser. The dye used in this laser was oxazine 720 ( $1 \times 10^{-4}$  M) in methanol. The optical resonator of the slave oscillator consists of a flat, 60% reflectivity output coupler and a flat, 90% reflectivity mirror. The 90% mirror serves as an input coupler for the narrow-band radiation from the injection laser. It was necessary to tune the free-running output of the slave oscillator to 706 nm by means of an intracavity Pellin-Broca prism to achieve efficient injection-locking of this laser.

Output from this dye laser system was typically 120 mJ in a  $0.2 \text{ cm}^{-1}$  wide line at 706 nm. Frequency doubling in an angle-tuned KDP crystal generated a useful 353 nm beam of about 0.5 mJ. An expanding telescope was used to match the injection beam to the mode diameter of the XeF laser.

Appropriate electrical timing delays were incorporated to insure that the excimer laser was triggered near the center of the 500 ns long uv injection pulse.

Figure 2 shows XeF laser spectra obtained with the 1 meter spectrometer with and without the presence of the narrowband injection signal. Line-narrowing and peak height enhancement effects are evident, although the injection-locked spectrum in Figure 2 is limited in resolution by the spectrometer. It should be noted

that a small peak on the long-wavelength side of the injection-locked spectrum is due to a low level contribution in the injection signal which arises from another transmission mode of the CMX-4 line-narrowing etalon. Figure 3, which shows data obtained with the Fabry-Perot etalon, depicts a cross sectional slice through the center of the Fabry-Perot ring pattern. The two tallest features are the first ring, while the smaller feature on the right is the second ring. Analysis of the Fabry-Perot spectrum shows that the locked laser linewidth is about  $0.3 \text{ cm}^{-1}$  or  $0.004 \text{ nm}$ . In Figure 2, the laser output power was about 570 kW, while the injection power was only 120 W. Thus a power ratio of 1:5000 was sufficient to control the spectral linewidth of the XeF laser. By utilizing better cavity mode-matching between the XeF laser and the injection beam, it should be possible to achieve locking at even lower injection intensities. Analysis of the laser intensity reflected from a  $45^\circ$  angle-fused silica beam splitter showed that the injection-locked XeF laser assumed the same polarization as the injection signal. This is similar to the results obtained by Pacala and Christensen<sup>6</sup> with a lower energy, shorter pulse length XeF laser.

Most of the energy output of this XeF laser lies in the 353 nm band (0,3 transition). A few percent of the output occurs at 351.1 nm (0,2 transition). No evidence of the 1,4 transition near 351.0 nm was observed. Since the laser is operated at room temperature with pulse lengths on the order of 100 ns, absence

of the 1,4 transition is expected.<sup>7</sup> With the injection source tuned to the 0,3 transition, the 0,2 transition disappears as expected. With the injection source tuned to the 0,2 transition, a large peak-height enhancement is observed at 351 nm with a partial depression of lasing on the 0,3 transition. It was not possible to significantly depress output on the 0,3 transition in the present experiment. These results indicate rotational relaxation in the B state of XeF which occurs on a time scale equal to or faster than the stimulated emission rate.

In addition to these experiments with the coaxial e-beam excited XeF laser, a larger XeF laser excited by a transverse e-beam<sup>8</sup> has also been injection-locked. In the present configuration, this laser had a gain volume of  $10 \text{ cm}^2$  by 100 cm long. The output energy was about 0.8 J in a  $1.2 \mu\text{s}$  long optical pulse. The same injection source shown in Figure 1 was used with this larger XeF laser. In this case, however, the temporal duration of the injection signal is less than the XeF laser pulse length. By timing the injection signal to occur early in the XeF laser pulse, the entire laser pulse could be injection-locked. Fabry-Perot spectra similar to that shown in Figure 3 indicate the injection-locked XeF laser linewidth is  $0.5 \text{ cm}^{-1}$  or 0.006 nm. As with the coaxial XeF laser, an injection power ratio of about  $10^{-5}$  was sufficient to control the laser linewidth. In both experiments described here, over 90% of the unlocked XeF laser output was present in the narrowband, injection-locked output.

In summary, we have demonstrated that the line-width and polarization of an XeF laser can be well controlled by the injection-locking technique. This method is efficient and scalable to larger devices. Presently, experiments are in progress to scale the technique to higher energy lasers, larger output apertures, and unstable resonator cavities. The authors wish to thank L. S. Azevedo, P. C. Stevens, and M. Hurst for their expert technical assistance in performing these experiments.

## REFERENCES

1. E. R. Ault, R. S. Bradford, Jr., and M. L. Bhaumik, Appl. Phys. Lett. 27, 413 (1975)
2. L. F. Champagne and N. W. Harris, Appl. Phys. Lett. 31, 513 (1977)
3. C. J. Buczek, R. J. Freiberg, and M. L. Skolnick, Proc. IEEE 61, 1411 (1973)
4. J. Goldhar, J. Dickie, L. P. Bradley, and L. D. Pleasance, Appl. Phys. Lett. 31, 677 (1977)
5. E. R. Ault, Appl. Phys. Lett. 26, 619 (1975)
6. T. J. Pacala and C. P. Christensen, Appl. Phys. Lett. 36, 620 (1980)
7. L. F. Champagne, Appl. Phys. Lett. 35, 516 (1979)
8. W. B. Lacina and D. B. Cohn, Appl. Phys. Lett. 32, 106 (1978)

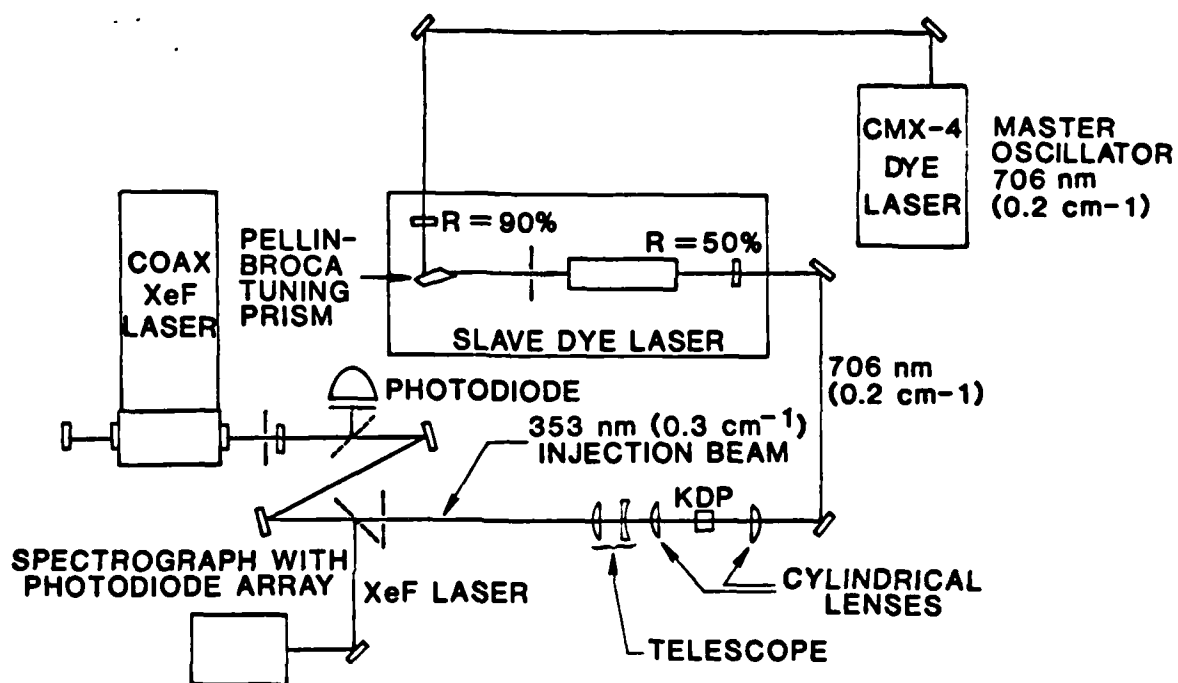


Figure 1. Experimental arrangement for XeF laser injection locking. The narrowband injection signal is derived from a frequency doubled dye laser.

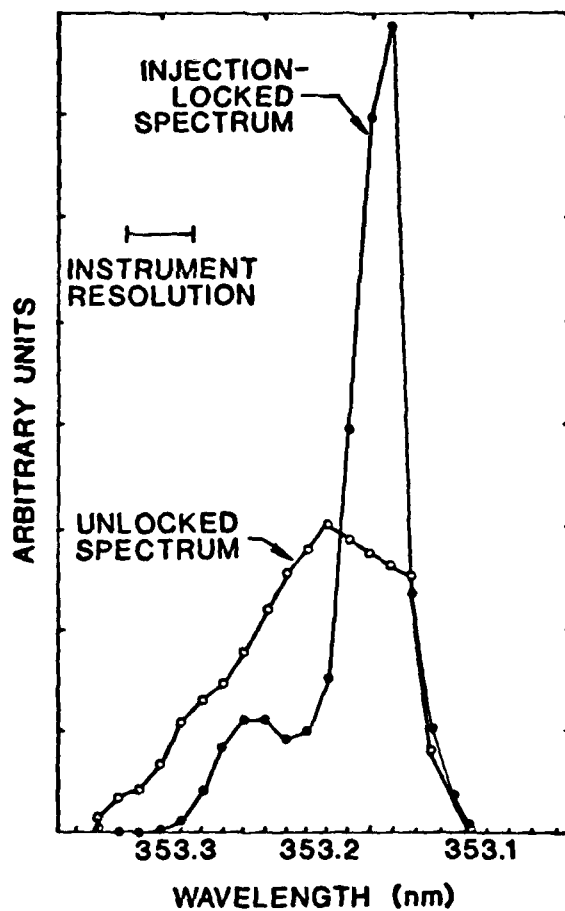


Figure 2. XeF laser spectrum with and without injection locking. The small peak on the long wavelength wing of the injection locked spectrum is due to a small, contaminating signal injected at that frequency.

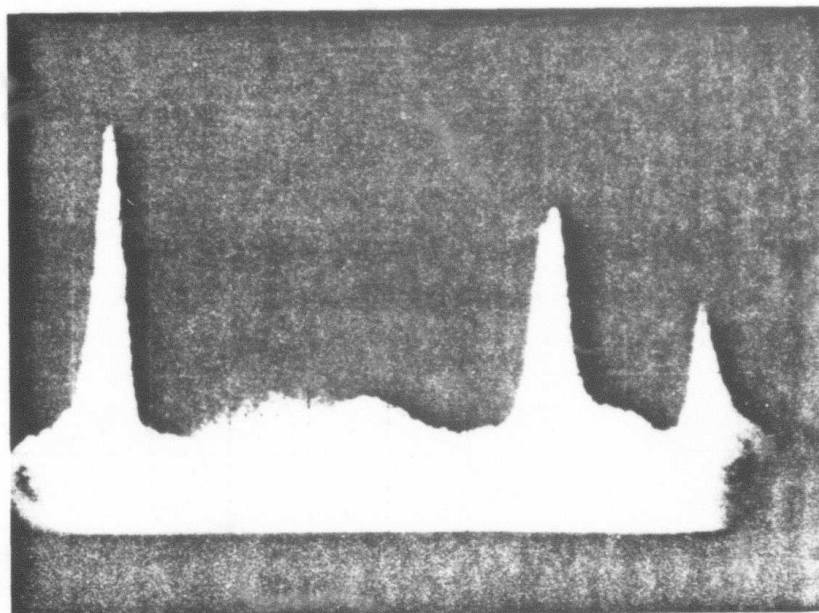


Figure 3. Fabry-Perot spectrum of injection locked XeF laser.  
Laser linewidth is  $0.3 \text{ cm}^{-1}$ .



## APPENDIX B

### EFFICIENT $H_2$ RAMAN CONVERSION OF LONG-PULSE XeF LASER RADIATION INTO BLUE-GREEN REGION\*

H. Komine, E. A. Stappaerts, S. J. Brosnan and J. B. West  
Northrop Corporation  
Northrop Research and Technology Center  
One Research Park  
Palos Verdes Peninsula, California 90274

#### ABSTRACT

Efficient Raman conversion of microsecond pulse XeF laser radiation into the blue-green region via the second Stokes shift in hydrogen has been demonstrated using a Raman oscillator-amplifier scheme. Strong depletion of the pump and the first Stokes radiation accompanied by a dominant second Stokes output was observed for the first time.

\* Work supported in part by DARPA/ONR contract No. N00014-80-C-0442.

EFFICIENT  $H_2$  RAMAN CONVERSION OF LONG-PULSE  
XeF LASER RADIATION INTO BLUE-GREEN REGION

H. Komine, E. A. Stappaerts, S. J. Brosnan  
and J. B. West

Efficient Raman shifting of ultraviolet excimer laser radiation has received considerable interest in the past several years as a means of generating high power coherent radiation in the near UV and the visible region.<sup>1-3</sup> Experimental demonstration of high conversion efficiencies has been reported for various atomic and molecular Raman media using relatively short UV pump pulses with low energies.<sup>4-6</sup> Currently, there exists a strong interest in extending the molecular Raman conversion process to higher energies and longer pulse lengths ( $> 1 \mu s$ ) with electron-beam pumped rare-gas halide lasers. A superfluorescent Raman oscillator with submicrosecond pulses of e-beam pumped XeF laser radiation<sup>7</sup> has indicated efficient first Stokes generation in high pressure hydrogen gas. We report, in this Letter, efficient  $H_2$  Raman conversion of XeF laser radiation with pulse lengths of up to one microsecond, in which the dominant output is observed in the second Stokes order (500 nm) for the first time using a Raman oscillator-amplifier configuration.

The motivation for using an oscillator-amplifier configuration is two-fold: it provides an efficient method of converting pump laser radiation into second Stokes output, and the technique allows energy scaling and beam quality control. An oscillator based on molecular gases such as  $H_2$  and  $D_2$  generates Stokes radiation consisting of first, second, and third (or more) orders differing in frequency by the corresponding number of Raman shifts. A tightly focused pump

beam is typically employed for an oscillator in order to achieve high Raman gains, well above the threshold level, that are necessary to generate multiple-order Stokes output. In this conventional geometry, the onset of four-wave mixing effects help to start the higher Stokes order generation but ultimately limit their conversion efficiencies to relatively low values. Furthermore, since most of the conversion processes occur close to the focal region, saturation of the Raman medium limits the amount of laser energy that can be handled by an oscillator. A large mode volume pumping geometry for a high gain oscillator would prevent medium saturation; however, large, unacceptable beam divergences of the Stokes radiation result in this case.

Addition of a Raman amplifier with modest gains over a large mode volume provides the solution for overcoming the energy handling, efficiency and beam quality problems inherent in a conventional oscillator. In this case an oscillator is pumped by a small fraction of the laser radiation and operated to yield multiple-order Stokes output which is used as a source of injection radiation into an amplifier. Collimated and co-propagating pump and injected Stokes beams in the amplifier lead to a sequential transfer of pump radiation into successive Stokes orders as they travel through the amplifier. Under certain injection levels and gains, the conversion process may be halted in principle at a particular Stokes order with a high efficiency. Experiments based on this concept have been performed with short pulses, and their results have been reported for the case of second and third Stokes shifting in  $H_2$  pumped by Nd:YAG laser third harmonic<sup>8</sup> (355 nm) and XeCl (308 nm) laser<sup>6</sup> radiation, respectively.

In order to extend the oscillator-amplifier experiment to longer pulses and higher energies, an e-beam pumped XeF laser was set up as a pump source. A

cylindrically symmetric confocal unstable resonator of magnification 2.4, with an output beam diameter of 12 cm was employed for this laser. The laser was operated with a gas mixture of Xe (0.3%),  $\text{NF}_3$  (0.1%), Ne (99.6%) at a total density of 3 amagats. A pair of anti-reflection (AR) coated fused silica windows separated the gas from the resonator mirrors. The XeF 353 nm emission from this device was injection-locked to a narrow bandwidth, frequency-doubled, flashlamp-pumped dye laser system. XeF laser output energies up to 10 J in a microsecond pulse have been obtained in this manner with a laser bandwidth of about  $0.5 \text{ cm}^{-1}$  (.006 nm). Injection locking performance is described elsewhere along with further details on the laser<sup>9</sup>. Although the injection laser was polarized, the XeF output was essentially unpolarized, mainly due to stress/strain induced birefringence in the AR windows.

The Raman converter optical layout is schematically shown in Figure 1. A beam splitter (BS) transmits 20% of the XeF output. Under typical operating conditions the laser produced about 7.5 J output in a pulse length of  $0.7 \mu\text{s}$  at half-power points. Thus the oscillator arm had approximately 1.5 J pump energy, of which about 1 J was incident on a Raman cell after passage through beam-reducing (BR) optics and an optical path delay line. The oscillator cell was a 2 meter stainless steel tube with near-normal incidence AR coated windows. Simultaneous generation of up to third Stokes was observed at a hydrogen gas density range of 7.8 to 9.2 amagats. The Stokes threshold was observed approximately 100 to 200 ns after the leading edge of the pump pulse, due to a gradual rise of the pump pulse. The Stokes beam was expanded (BX) and transmitted through a beam-combining (BC) dielectric mirror which was coated for high reflectance at 353 nm and 70 ~ 80% transmittance at both 414 nm (first Stokes,  $S_1$ ) and 500 nm (second Stokes,  $S_2$ ). Measurements of Stokes injection indicated typical values around 100 mJ ( $S_1$ ), 20 mJ ( $S_2$ ) and <1 mJ ( $S_3$ ). These correspond to useful injection

intensities of approximately 2% ( $S_1$ ) and 0.5% ( $S_2$ ) relative to the pump intensity at the entrance of the amplifier.

The amplifier cell was 5.8 meters long and nominally contained 7.8 amagats of  $H_2$ . The fused silica input window was uncoated and tilted at  $3^\circ$  to the incident beam. The output window was an uncoated fused silica blank, tilted at  $45^\circ$  to the beam. To establish requisite gains in the amplifier, the pump beam was reduced to a diameter of 1.2 cm with lenses  $L_1$  and  $L_3$ , and a gain-enhancement technique was then utilized to optimize the multimode Raman gain. For the gain-enhancement alignment, 10 pps Nd:YAG laser third harmonic radiation was introduced before the first beam splitter to simulate the XeF laser. This permitted a real-time temporal matching of the arrival of the pump and injected Stokes pulses in the amplifier. A variable optical path delay line in the oscillator arm provided the necessary adjustments to optimize the Raman gain. Based on the measured beam size and pump power, an estimated amplifier gain for the first Stokes is approximately  $e^{16}$  for each polarization component.

Raman amplifier conversion was monitored by a group of three vacuum photodiodes (ITT F4000) and three Gentec ED500 pyroelectric joule meters for each of the  $S_1$  and  $S_2$  and depleted pump beams after they were dispersed by a Brewster angle prism. A separate photodiode also monitored the input pump pulse, which enabled a correlation between the pulse energy and the pulse shape. A representative set of photodiode traces of pump and Stokes outputs is shown in Figure 2. These traces correspond to cases in which the  $S_2$  output dominated over the  $S_1$  output. Figure 2(a) is a trace which was taken without  $H_2$  gas, and it represents an undepleted pump pulse. Figure 2(b) shows a typical depleted pump pulse with Raman conversion. Energy measurements, referenced to the entrance and the output in the amplifier medium, indicate 5.1 J at the entrance and 1.2 J left over at

the output end. These values yield a typical pump depletion near 75%. Figure 2(c) and 2(d) show  $S_1$  and  $S_2$  pulses, respectively, for the same conditions as in Figure 2(b). The measured energies corrected for exit-window transmission are 1.2 J ( $S_1$ ) and 1.7 J ( $S_2$ ). A substantial sustained depletion of the  $S_1$  pulse is clearly evident in Figure 2(c) which explains a larger output for  $S_2$ . These data show a 34% energy and 43% peak power conversion into the second Stokes. To our knowledge, these data represent the highest efficiency figure as well as the largest energy output to date for long pulse XeF Raman conversion into the blue-green. It is also noteworthy that the photon conversion efficiencies are 28% ( $S_1$ ) and 47% ( $S_2$ ), clearly demonstrating a selective conversion process in the amplifier for the desired Stokes order. Similar efficiencies were also observed for pulse lengths up to 1  $\mu$ s, which was the longest optical pulse length of the XeF laser used in these experiments.

In a series of preliminary parametric experiments, amplifier performance dependence on  $H_2$  pressure and pump intensities was investigated. As the pump intensities are reduced, thereby diminishing the gain, the  $S_2$  conversion efficiency decreased while the  $S_1$  efficiency increased, in good agreement with our model calculations which predict a more favorable  $S_1$  conversion at lower gains. Reduction in  $H_2$  density also reduces the gain for the density range of 3 to 8 amagats used in the experiment. As expected, the  $S_1$  efficiency increased and the  $S_2$  efficiency decreased at lower  $H_2$  densities at a given pump intensity. This behavior was compensated with an increase in the pump intensity, as predicted. This observation indicates that  $H_2$  density variation can be used to fine-tune amplifier gains. A more detailed parametric investigation is in progress to characterize the amplifier performance, including polarization dependence and beam quality.

In summary, we have demonstrated efficient and selective second Stokes conversion of long pulse XeF (353 nm) laser radiation into 500 nm blue-green output using an H<sub>2</sub> Raman oscillator-amplifier configuration. The measured energy and peak power conversion efficiencies in the amplifier suggest that Raman converters based on this concept should be scalable to high energies with respectable efficiencies, making them interesting for a wide range of applications.

The authors wish to express their gratitude to Messrs. P. C. Stevens and S. Azevedo for their technical assistance in the laboratory.

## REFERENCES

1. N. Djeu and R. Burnham, Appl. Phys. Lett. 30, 473 (1977)
2. T. R. Loree, R. C. Sze, and D. L. Barker, Appl. Phys. Lett. 31, 37, (1977)
3. T. R. Loree, R. C. Sze, D. L. Barker, and P. B. Scott, IEEE J. Quant. Electron. QE-15, 337 (1979)
4. D. Cotter and W. Zapka, Opt. Commun. 26, 251 (1978)
5. R. Burnham and N. Djeu, Opt. Lett. 3, 215 (1978)
6. H. Komine and E. A. Stappaerts, Paper EE-8, International Lasers '80 Conference Proceedings (December 15 - 19, 1980)
7. D. W. Trainor, H. A. Hyman, I. Itzkan, and R. M. Heinrichs, Appl. Phys. Lett. 37, 440 (1980)
8. H. Komine and E. A. Stappaerts, Opt. Lett. 4, 398 (1979)
9. J. B. West, H. Komine, and E. A. Stappaerts, J. Appl. Phys. 52, 5383 (1981)



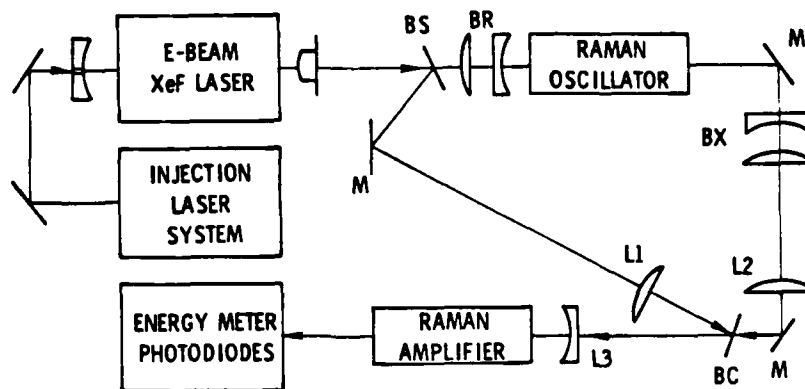
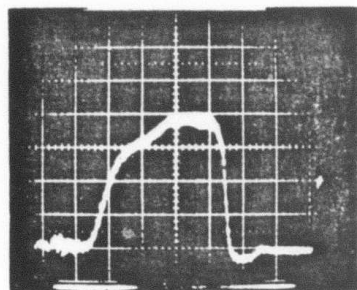


Figure 1. Experimental Schematic:

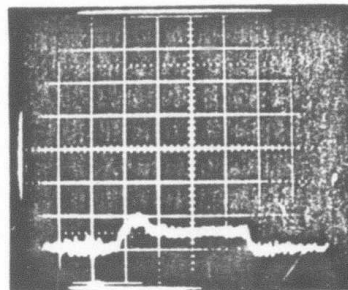
BS = Beam Splitter; BR = Beam Reducing Optics;

M = Mirror; BX = Beam Expander Optics;

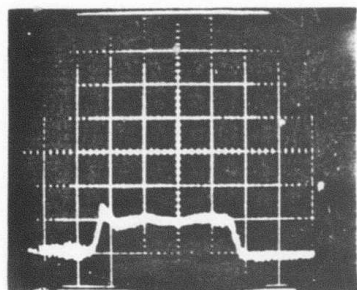
BC = Beam Combining Dichroic Mirror; L1, L2, L3 = Lenses



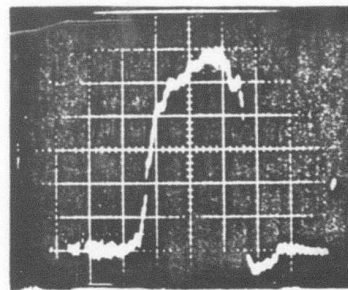
(a)



(c)



(b)



(d)

Figure 2. Photodiode Traces of Pump Depletion and Stokes Amplification  
in Raman Amplifier:

- (a) Undepleted Pump
- (b) Depleted Pump
- (c) Amplified First Stokes
- (d) Amplified Second Stokes

(0.2  $\mu$ s/div. horiz. scale; arb. units vert. scale;  
only (a) and (b) have the same vertical scale).